

# *Zonyl FSP fluorosurfactant stabilized perfluorohexane nanoemulsions as stable contrast agents*

Donald A. Fernandes<sup>1,3,4</sup> and Michael C. Kolios<sup>1,2,3,4,\*</sup>

<sup>1</sup>Department of Chemistry & Biology, Ryerson University, Toronto M5B 2K3, Canada.

<sup>2</sup>Department of Physics, Ryerson University, Toronto M5B 2K3, Canada.

<sup>3</sup>Institute for Biomedical Engineering, Science and Technology (iBEST), a partnership between Ryerson University and St. Michael's Hospital, Toronto, Ontario M5B 1T8, Canada.

<sup>4</sup>Keenan Research Centre for Biomedical Science of St. Michael's Hospital, Toronto, Ontario M5B 1T8, Canada.

\*mkolios@ryerson.ca

**Abstract**— Nanoemulsions have been used as theranostic agents for both imaging cancer, (using various imaging modalities) as well as for therapy through drug loading/release and vaporization. However, some of these imaging contrast agents are not stable enough to be used for long term monitoring of tumor growth/regression during therapy. When used *in vivo*, several nanoparticle agents rely on the use of optical absorbers which may have systemic toxicity. The current work uses perfluorohexane nanoemulsions (PFH-NEs) stabilized by a highly biocompatible optically absorbing fluorosurfactant shell that can be used to not only give stable PA signals but also enhance signals through the presence of long lasting perfluorohexane (PFH) bubbles formed after vaporization.

**Keywords**— *photoacoustic, nanoemulsions, phase-change contrast agents*

## I. INTRODUCTION

Over the last few decades nanotechnology has emerged as a promising field in the development of theranostic agents for both monitoring tumor progression/regression as well as for treating malignant tumors. For example, nanoparticles can be synthesized to carry a variety of fluorescent imaging agents as well as load a variety of therapeutic agents, including those that are naturally hydrophobic and insoluble for therapy [1-4]. The ability of fluorescent nanoparticles to release heat upon laser irradiation has led to synergistic effects leading to further cancer death using drug loaded and fluorescent nanoparticles [5,6]. Theranostic agents have also been used in other imaging modalities such as MRI [7] and ultrasound (US) [8] due to advantages such as greater penetration depth, sensitivity and contrast compared to other imaging modalities. One imaging modality which is comparable to MRI and US is photoacoustic

(PA) imaging. Compared to other optical imaging techniques, PA imaging provides greater penetration depth (due to the detection of acoustic waves) and sensitivity, being able to detect acoustic waves from the expansion of highly optically absorbing regions/contrast agents in tissue [9].

This study shows how perfluorocarbon nanoemulsions, stabilized by a negatively charged fluorosurfactant shell (Zonyl FSP) can be used as contrast agents [10-13]. The ability of the shell to absorb near-infrared light leads to vaporization of the perfluorohexane (PFH) core leading to the formation of bubbles. The expansion of nanodroplets (PFH-NEs) into nanobubbles and microbubbles leads to the generation of acoustic waves which can be detected and used for imaging of breast cancer cells. The stable nanobubbles and microbubbles formed can be used as contrast agents in contrast enhanced ultrasound (CEUS) imaging. To characterize size and morphology of PFH-NEs, dynamic light scattering (DLS) and transmission electron microscopy (TEM) was used, with the therapeutic ability and photoacoustic properties demonstrated using a commercial photoacoustic imaging system (Vevo LAZR).

## II. MATERIALS AND METHODS

### A. Synthesis and Characterization of Fluorosurfactant coated PFH-NEs and Bubbles

Perfluorohexane nanoemulsions (PFH-NEs) were synthesized by first mixing vigorously, 300  $\mu$ l of PFH (1100-2-07, Synquest Laboratories), 150  $\mu$ l of Zonyl FSP fluorosurfactant (09988, Sigma-Aldrich) and 4250  $\mu$ l of Milli-Q water prior to sonication (20 kHz) on ice for 2 minutes (10 s

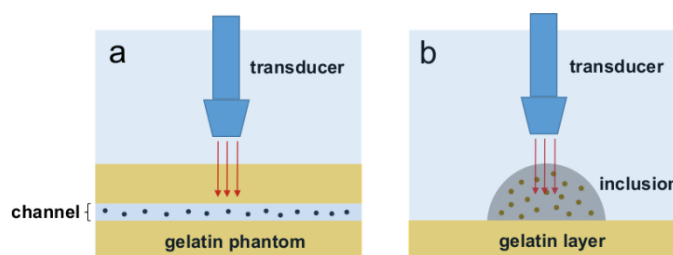
on/ 20 s off), at 20% amplitude (11 Watts). The morphology of PFH-NEs was characterized using transmission electron microscopy (TEM) by placing a few drops of NEs on a TEM grid. A TEM voltage of only 80 kV was used to minimize excess heating of the sample and vaporization of PFH-NEs into bubbles. Also, since the NEs contain electron dense fluorine atoms, the NEs could be imaged under TEM without the addition of an external label for distinguishing NEs. To acquire a more accurate representation of size of NEs in their aqueous environment, dynamic light scattering (DLS, Brookhaven 90Plus Particle Size Analyzer) was used, which converts the scattered signals from NEs with time into an autocorrelation function and size distribution [14].

### B. Photoacoustic and Ultrasound Imaging of PFH-NEs and Bubbles

To characterize the ability of PFH-NEs to vaporize into PFH bubbles and generate ultrasound and photoacoustic signals, a Vevo LAZR (FUJIFILM VisualSonics Inc.) commercial imaging system was used. The PFH-NEs were mixed with 10% weight/volume gelatin (Type A, 250 Bloom, G2500, Sigma-Aldrich) to create inclusions or placed in channels (Schematic 1). The NEs were then vaporized using 700 nm laser excitation at 20 mJ/cm<sup>2</sup> laser fluence, from a tunable (680-970 nm) Nd:YAG laser, with a repetition rate of 20 Hz and pulse duration of 4-6 ns. Prior to photoacoustic imaging, PFH-NEs were imaged using ultrasound with a 21 MHz transducer, a focusing depth of 11 mm and only 1% US power (to minimize vaporization). Next, to show the biomedical application of NEs for imaging cancer cells, PFH-NEs were incubated (at non-cytotoxic concentrations determined using trypan blue viability dye) with MCF-7 breast cancer cells (ATCC). MCF-7 cells at a concentration of 125,000 cells/mL were initially grown in T-25 flasks for 24 hours in Dulbecco's Modified Eagle Media (DMEM) (comprising 4500 mg glucose/L, L-glutamine, NaHCO<sub>3</sub>, and sodium pyruvate with 10 % fetal bovine serum). The PFH-NEs were then added and incubated with cells for 4, 24 or 48 hours before washing cells and trypsinization. The NEs loaded cells were then mixed with 10% w/v gelatin and imaged using the Vevo LAZR (at 700 nm laser excitation) at the above experimental conditions (at 37°C). All concentrations of NEs used with cells were found to cause no cytotoxicity using the trypan blue viability dye.

For determining stability, the NEs and PFH bubbles were imaged in gelatin inclusions (as mentioned above, Schematic 1) at day 0 and day 1 (or 24 hours) after incubation of NEs and bubbles at 37°C in a water bath (between measurements). On each day, PFH-NEs/bubbles were excited for 10 seconds at 700 nm using Vevo LAZR to determine the stability of PA and US signals with time. Contrast mode on the Vevo LAZR was used with nonlinear contrast enhanced ultrasound (NL CEUS) to quantify the signals from bubbles after 10 seconds vaporization of NEs on each day. Average signals represented for NL US are from 1 mm x 3 mm regions at the centers of inclusions using ImageJ. To compare signals from PFH-NEs, PFH-NEs with

silica coated gold nanoparticles (scAuNPs) were used using the same previous procedures for making such nanoparticles [10] and excitation at 680 nm. For each type of experiment, the same imaging parameters were kept constant (*i.e.*, US and PA gain) in order to determine trends in the signals. All averages reported for US and PA signals (mean ± standard deviation from three replicates) are from the mean from the absolute values of amplitudes from Hilbert transformed data (from more than 25 radio-frequency lines per replicate) using MATLAB codes for analysis. Unless otherwise stated, all signals represented are for nanoparticles and bubbles directly after excitation (at frame 1).



Sch. 1. **Experimental setup for imaging.** Illustration of how samples were made for US and PA experiments in gelatin channels (a) or inclusions (b) consisting of nanoparticles/bubbles or cells with nanoparticles/bubbles. Experiments were carried out using the Vevo LAZR with laser excitation from the top of inclusions and channels.

## III. RESULTS AND DISCUSSION

### A. Size and Morphology of PFH-NEs

The size of PFH-NEs was monodisperse with the size distribution being unimodal, determined using dynamic light scattering (DLS) (Figure 1 a). Furthermore, as seen under TEM, the PFH-NEs are spherical, containing electron dense fluorine atoms both on their shell and core (Figure 1 b). Because the PFH-NEs are between 10-500 nm, they are able to exploit the unique characteristics of the tumor microenvironment (*i.e.*, large endothelial gaps up to 1-2 μm in size) for effective accumulation at the tumor [15,16] and are neither very small or big, avoiding clearance by the reticuloendothelial system (RES) and the kidneys, liver and spleen.

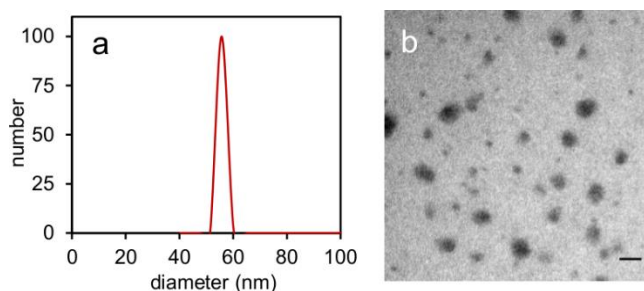


Fig. 1. **Characterization of PFH-NEs.** Size distribution of perfluorohexane nanoemulsions measured by dynamic light scattering (DLS) (a) and a representative transmission electron microscope image (b) of PFH-NEs consisting of electron dense fluorine atoms (scale bar: 50 nm).

### B. Ultrasound (US) and Photoacoustic (PA) Signals from PFH-NEs

To determine whether PFH-NEs could give PA signals from vaporization of nanodroplets the Vevo LAZR was used at 700 nm. After near-infrared laser excitation, the vaporized PFH-NEs gave significant PA and US signals (Figure 2 a and b). The US signals increased due to the number of PFH bubbles formed from vaporization or from an increase in the concentration of NEs (Figure 2 c). This also resulted in an increase in the PA signals due to increase in the number of vaporization events with concentration (Figure 2 d). The signals from PFH-NEs were also found to be stable with repeated laser excitation after 4 minutes (Figures 2 e,f) showing the potential of these contrast agents to be used for long term imaging where stability is important.

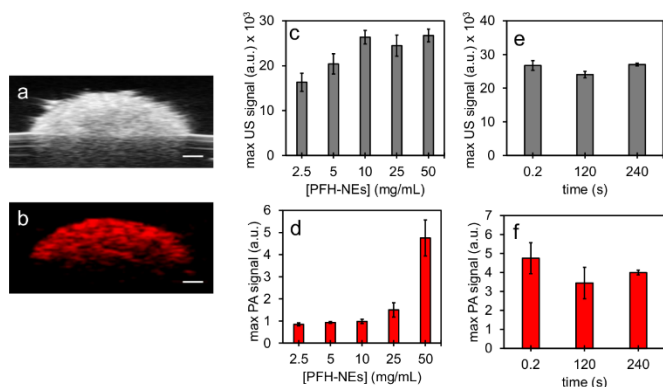


Fig. 2. PA and US signals from PFH-NEs. US (a) and PA (b) images of vaporized PFH-NEs (from 50 mg/mL solution of PFH-NEs) directly after 700 nm laser excitation (at frame 1) using Vevo LAZR with US (c) and PA (d) signals with different concentrations of PFH-NEs. All measurements carried out at 25°C in gelatin phantoms (scale bar: 1 mm). Stability of US (e) and PA (f) signals are shown with time for 50 mg/mL solution of NEs.

Furthermore, to determine the ability of PFH-NEs to give US and PA signals at physiological conditions (*i.e.*, 37°C with cells), nanoparticles were vaporized after incubation with MCF-7 cancer cells (after 4, 24 and 48 hours). Signals from PFH-NEs were located throughout the cell inclusion (Figure 3), suggesting the ability of NEs to efficiently attach and/or internalize in cells. PA signals were found to be constant with time with signal values of  $4.33 \pm 1.14$ ,  $5.51 \pm 0.26$  and  $4.91 \pm 0.73$  after 4, 24 and 48 hours respectively, suggesting that the PFH-NEs are stable and can be used for biomedical applications for imaging of tumor progression/regression.

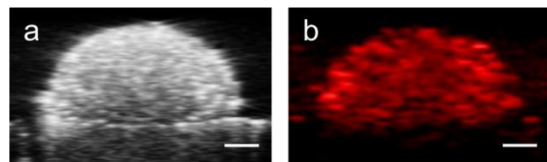


Fig. 3. PA and US image from vaporization of PFH-NEs in cancer cells embedded in gelatin phantoms. US (a) and PA (b) images (after 4 hours incubation of particles with cells) of vaporized PFH-NEs (from 10 mg/mL solution of PFH-NEs). All measurements carried out at 37°C (scale bar: 1 mm).

As the PFH-NEs can form PFH bubbles upon laser excitation, the US and PA signals were detected at days 0 and 1 to determine whether the formed bubbles were stable and could enhance PA signals after 24 hours. The PA signals were enhanced more than 20 times (PA signal  $25.6 \pm 10.1$  (a.u.)) compared to PA signals from vaporization of NEs at day 0 (PA signal  $1.3 \pm 0.1$  (a.u.)) (Figure 4 a,b,e). This suggests that the increase in signals might be due to the presence of greater and/or bigger stable bubbles due to coalescence of smaller bubbles which are only present after vaporization of NEs (Figure 5).

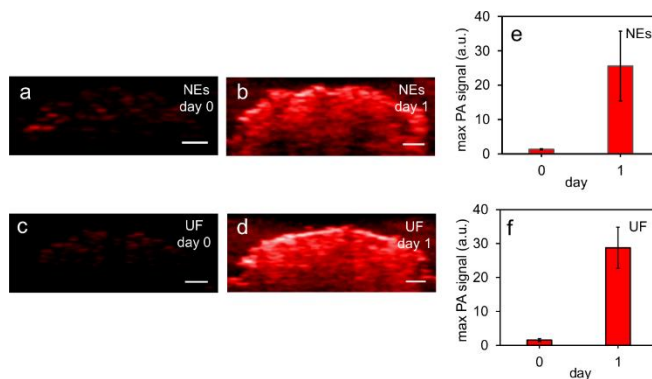


Fig. 4. PA and US signals from PFH-NEs at day 0 and 1. PA images (a-d) and signals (e,f) from vaporized PFH-NEs and PFH-NEs with 0.75 µg/mL silica coated gold nanoparticles (UF nanoparticles) (both samples using 5 mg/mL solution of PFH-NEs) at day 0 and 1 (scale bar: 1 mm). All measurements carried out at 37°C.

This can also be seen from nonlinear ultrasound imaging results from the increase in signals at day 1 compared to day 0 (Figure 6). These bubbles likely amplify signals for PA imaging due to their ability to increase acoustic scattering of the photoacoustic ultrasound waves produced. Because of the presence of both microbubbles and nanobubbles determined in previous experiments [17,18], the bubbles generated from vaporization of NEs can significantly enhance the PA signals due to greater scattering. The signals from NEs alone were even comparable to NEs with silica coated gold nanoparticles (Figure 4 c,d,f), a common optical absorber. Results show the ability of PFH bubbles from NEs to be used as multimodal contrast agents, especially for NL CEUS imaging, which is more sensitive towards detecting signals from nonlinear oscillations of bubbles compared to the surrounding tissue [19].

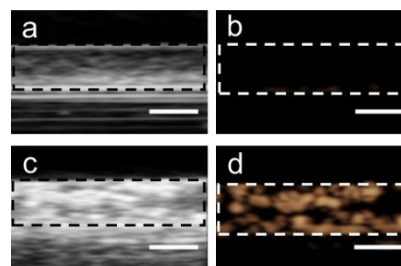


Fig. 5. US and NL CEUS images from PFH-NEs and PFH bubbles. Linear US (a, c) and NL US (b, d) images before (a, b) and after (c, d) vaporization at 700 nm (from 20 mg/mL solution of PFH-NEs). All measurements carried

out at 37°C (scale bar: 1 mm). Increase in US and NL CEUS signals after vaporization are due to the presence of PFH bubbles.

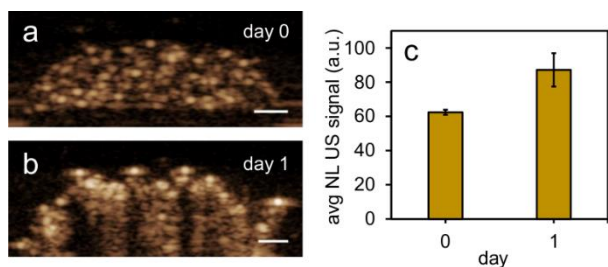


Fig. 6. NL CEUS signals from PFH-NEs at day 0 and 1. NL US images (a,b) and signals (c) from PFH-NEs (using 5 mg/mL solution of PFH-NEs) at day 0 and 1 (scale bar: 1 mm) after vaporization at 700 nm. All measurements carried out at 37°C.

#### IV. CONCLUSIONS

Stable PFH-NEs were synthesized for cancer theranostics by surrounding perfluorohexane nanoemulsions with a surfactant Zonyl FSP shell. The PFH-NEs were stable even after 48 hours incubation with MCF-7 cancer cells suggesting their stability at physiological conditions. One unique characteristic of these contrast agents is that the bubbles formed from vaporized NEs are stable and can be used for imaging even after 24 hours, amplifying PA signals most likely due to scattering from bubbles formed after vaporization.

#### ACKNOWLEDGMENTS

This work was supported by grants from the Canadian Institutes of Health Research (CIHR) and CFI (Canada Foundation for Innovation). D.A.F was supported by a Ryerson Graduate Fellowship.

#### REFERENCES

[1] M. Kester, Y. Heikal, T. Fox, A. Sharma, G. P. Robertson, T. T. Morgan, *et al.*, "Calcium phosphate nanocomposite particles for in vitro imaging and encapsulated chemotherapeutic drug delivery to cancer cells," *Nano letters*, vol. 8, pp. 4116-4121, 2008.

[2] T. Yildiz, R. Gu, S. Zauscher, and T. Betancourt, "Doxorubicin-loaded protease-activated near-infrared fluorescent polymeric nanoparticles for imaging and therapy of cancer," *International journal of nanomedicine*, vol. 13, p. 6961, 2018.

[3] Y. Zhang, C. Wei, F. Lv, and T. Liu, "Real-time imaging tracking of a dual-fluorescent drug delivery system based on doxorubicin-loaded globin-polyethylenimine nanoparticles for visible tumor therapy," *Colloids and Surfaces B: Biointerfaces*, vol. 170, pp. 163-171, 2018.

[4] G. Bao, S. Mitragotri, and S. Tong, "Multifunctional nanoparticles for drug delivery and molecular imaging," *Annual review of biomedical engineering*, vol. 15, pp. 253-282, 2013.

[5] C.-Y. Lin and M.-J. Shieh, "Near-Infrared Fluorescent Dye-Decorated Nanocages to Form Grenade-like Nanoparticles with Dual Control Release for Photothermal Theranostics and Chemotherapy," *Bioconjugate chemistry*, vol. 29, pp. 1384-1398, 2018.

[6] S. Hameed, P. Bhattarai, X. Liang, N. Zhang, Y. Xu, M. Chen, *et al.*, "Self-assembly of porphyrin-grafted lipid into nanoparticles encapsulating doxorubicin for synergistic chemo-photodynamic

therapy and fluorescence imaging," *Theranostics*, vol. 8, p. 5501, 2018.

[7] Y. Jeong, H. S. Hwang, and K. Na, "Theranostics and contrast agents for magnetic resonance imaging," *Biomaterials research*, vol. 22, p. 20, 2018.

[8] F. Kiessling, S. Fokong, J. Bzyl, W. Lederle, M. Palmowski, and T. Lammers, "Recent advances in molecular, multimodal and theranostic ultrasound imaging," *Advanced drug delivery reviews*, vol. 72, pp. 15-27, 2014.

[9] S. Park, U. Jung, S. Lee, D. Lee, and C. Kim, "Contrast-enhanced dual mode imaging: photoacoustic imaging plus more," *Biomedical engineering letters*, vol. 7, pp. 121-133, 2017.

[10] D. A. Fernandes, D. D. Fernandes, Y. Li, Y. Wang, Z. Zhang, D. r. Rousseau, *et al.*, "Synthesis of stable multifunctional perfluorocarbon nanoemulsions for cancer therapy and imaging," *Langmuir*, vol. 32, pp. 10870-10880, 2016.

[11] D. A. Fernandes, D. D. Fernandes, Y. J. Wang, Y. Li, C. C. Gradinaru, D. Rousseau, *et al.*, "Multifunctional perfluorocarbon nanoemulsions for cancer therapy and imaging," in *Colloidal Nanoparticles for Biomedical Applications X*, 2015, p. 93380R.

[12] D. A. Fernandes, D. D. Fernandes, C. C. Gradinaru, and M. C. Kolios, "In Vitro Studies of Multifunctional Perfluorocarbon Nanoemulsions for Cancer Therapy and Imaging," *Biophysical Journal*, vol. 110, p. 503a, 2016.

[13] D. A. Fernandes, D. D. Fernandes, Y. J. Wang, Y. Li, C. C. Gradinaru, D. Rousseau, *et al.*, "Phase Change Nanoemulsions for Cancer Therapy and Imaging," *Biophysical Journal*, vol. 108, pp. 332a-333a, 2015.

[14] J. Stetefeld, S. A. McKenna, and T. R. Patel, "Dynamic light scattering: a practical guide and applications in biomedical sciences," *Biophysical reviews*, vol. 8, pp. 409-427, 2016.

[15] R. K. Jain, "Taming vessels to treat cancer," *Scientific American*, vol. 298, pp. 56-63, 2008.

[16] V. Torchilin, "Tumor delivery of macromolecular drugs based on the EPR effect," *Advanced drug delivery reviews*, vol. 63, pp. 131-135, 2011.

[17] D. A. Fernandes and M. C. Kolios, "Intrinsically absorbing photoacoustic and ultrasound contrast agents for cancer therapy and imaging," *Nanotechnology*, vol. 29, p. 505103, 2018.

[18] D. A. Fernandes and M. C. Kolios, "Near-infrared absorbing nanoemulsions as nonlinear ultrasound contrast agents for cancer theranostics," *Journal of Molecular Liquids*, 2019.

[19] S. R. Wilson, L. D. Greenbaum, and B. B. Goldberg, "Contrast-enhanced ultrasound: what is the evidence and what are the obstacles?," *American Journal of Roentgenology*, vol. 193, pp. 55-60, 2009.